CHAPTER 2

BACKGROUND THEORY

2.1 Seismic Inversion

The popularity in seismic inversion techniques has been increasing highly for the last two decades due to the capability in delivering insightful reservoir characterization for hydrocarbon development projects. The results of inversion volume are closely related to rock properties of interest such as lithology, porosity and pore-fluid fill. Furthermore, the wavelet complexity such as tuning effect is diminished yielding simpler interface model.

Theoretically, inversion of seismic data is the process to produce an estimate of earth's acoustic and/or elastic impedances in several circumstances. This technique replaces the seismic reflectivity by a blocky response, corresponding to impedance layering (**Figure 2.1**). Reflectivity (R) is simply defined as the impedance contrasts across interface at normal incidence angle (zero-offset). The equation is expressed below:

$$R = \frac{Zp_{i+1} - Zp_i}{Zp_{i+1} + Zp_i,} \qquad \text{(Equation 2.1)}$$

where the impedance (Zp) is the product of velocity and density in the i^{th} layer.

In detail, acoustic impedance or P- impedance (Zp) is the product of density and P-wave velocity, and S-impedance (Zs) is the product of density and S-wave velocity. Elastic impedance is the product of density, P-wave velocity and S-wave velocity for variable angles of incidence, which would be discussed later.

By rearranging the terms of Equation 2.1, the series of impedance can be expressed as:

$$Zp_{i+1} = Zp_i\,[\,(1+R)/(1-R)], \qquad \text{(Equation 2.2)}$$

where R and Zp are zero-offset reflectivity and P-wave impedance respectively.

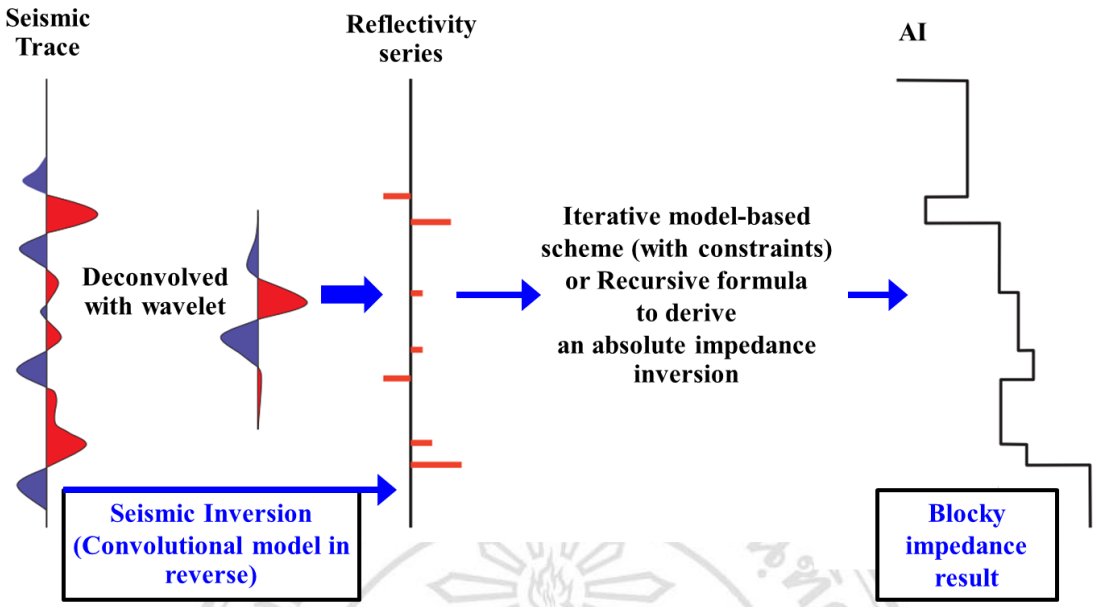

Figure 2.1 The concept of seismic trace inversion converted to impedance (modified from Simm and Bacon, 2014).

In other ways, the non-zero offset reflectivity (Rpp) can be given by the Aki and Richards's equation (1980) which is a linear approximation of Zoeppritz (1919) equations involving density (ρ), P-wave and S-wave velocities (Vp and Vs), and angle of incidence (θ). It is commonly used in the industry that is expressed below (Aki and Richards, 1980):

$$Rpp\ (\theta) = A + B.\sin^2\theta + C.(\sin^2\theta.\tan^2\theta), \qquad \text{(Equation 2.3)}$$

where θ = the angle of incidence,

$A = 0.5[(\Delta Vp/Vp)+(\Delta\rho/\rho)]$,

$B = 0.5(\Delta Vp/Vp) - \{2(\Delta Vs/Vp)^2.[2(\Delta Vs/Vs) + (\Delta\rho/\rho)]\}$,

$C = 0.5(\Delta Vp/Vp)$.

Vp, Vs, and ρ are the average properties from two interfaces (Vp = [Vp1 + Vp2]/2, Vs = [Vs1 + Vs2]/2, and ρ = [ρ1 + ρ2]/2) and Δ denotes the differences in the properties across the interface (ΔVp = Vp2 – Vp1, ΔVs = Vs2 – Vs1, and Δρ = ρ2 – ρ1).

The A term is the zero-offset reflectivity (or R in Equation 2.1) related to the contrast of acoustic impedance. The B term presents the effect of S-wave velocity at non-zero angles (Simm and Bacon, 2014). The last C term introduces the curvature of amplitude

(energy) response near to the critical angle (**Figure 2.2**). In this study on the amplitude versus offset (AVO) analysis, the A and B terms would be called in other names as intercept and gradient respectively.

In **Figure 2.2**, the critical angle is remarkably highlighted at each which is a particular angle in beginning of refraction effect. To be aware, as stated by Simm and Bacon, 2014, reflected P-wave energy beyond the critical angle would not be used because of the phase reversal and much more energy occur.

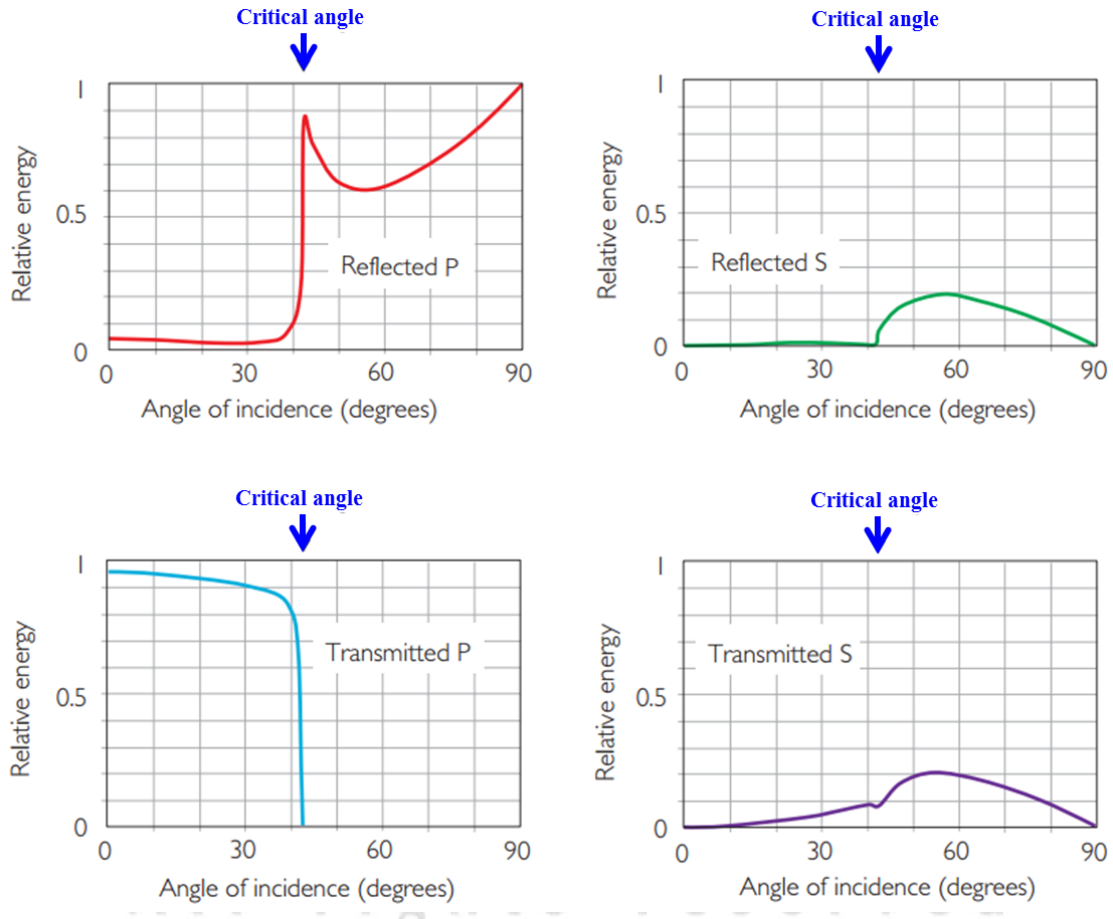

Figure 2.2. Schematic showing the expression of critical angle from the P-wave energy model at a single shale/limestone interface (modified from Simm and Bacon, 2014).

In principle, the inversion techniques can apply to both post- and pre-stack seismic data with the general use of migrated time as basic input and the methods are either deterministic or probabilistic. The examples of deterministic methods are simple integration of the seismic traces, sparse spike inversion, coloured inversion, and model-

based inversion (Veekan and Silva, 2004). In pre-stack seismic inversion, the amplitude variation with offset (AVO) effects on migrated common midpoint (CMP) gather would be considered and it is a trade-off between method/cost/time and quality of inversion results (Veekan and Silva, 2004).

Because of the bandwidth reduction in conventional seismic data, complement of low frequency component using P-wave sonic log, for example, could assure a more realistic result (Gavotti, 2014). The seismic inversion produces non-uniqueness results which mean there is no single solution to the given problem. On the other hand, there are a number of geological models consistent with the same seismic response. From time to time, the model-based inversion method becomes popular due to the iterative procedure of forward modeling and comparison (**Figure 2.3**). The model-based inversion method can ensure that the inversion result is not misleading, which produces geologically realistic solutions that correlate better with well control. This method will be applied in this study.

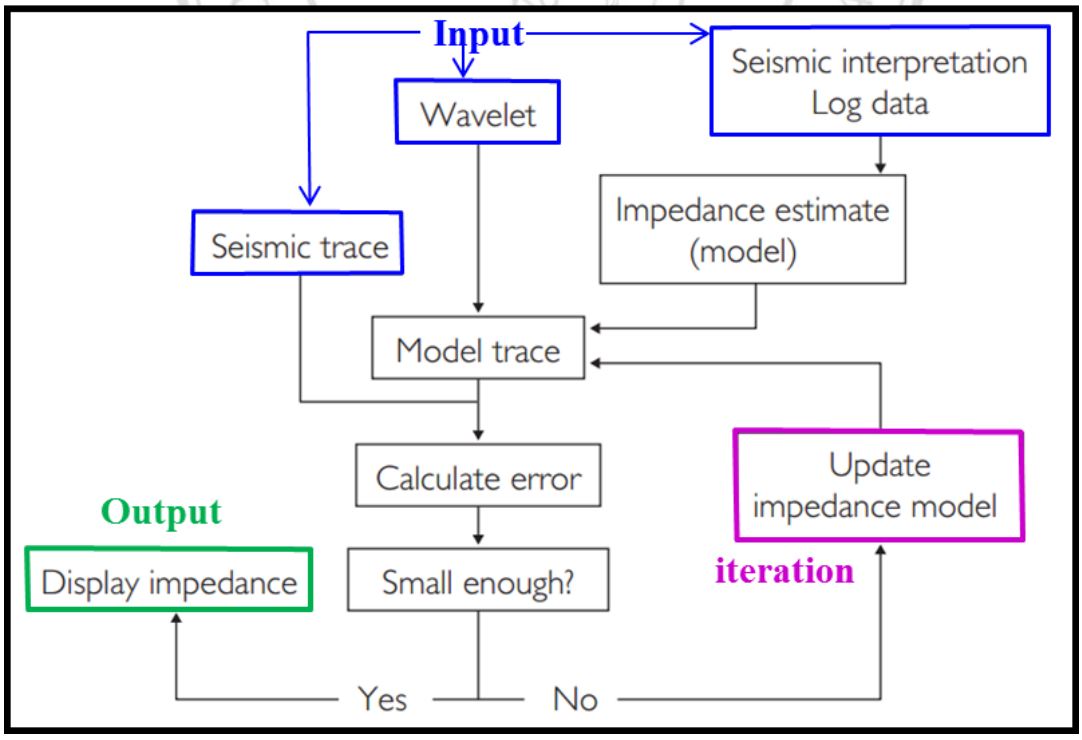

Figure 2.3. Schematic showing the procedure of model-based inversion method (modified from Simm and Bacon, 2014).

In the post-stack seismic inversion (i.e. the transformation of reflectivities to impedance at zero offset), it delivers only P-impedance result which can be used to discriminate lithology and porosity (Russell and Hampson, 2006). However, P-impedance principally affects by the variations in lithology, fluid, and porosity; thus it is difficult to discriminate in several circumstances. The pre-stack seismic inversion in conjunction with AVO technique aids this ambiguity by producing P-impedance, S-impedance and density which provide the great tool for lithology and fluid discrimination (Veekan and Silva, 2004; Avseth et al., 2005; Russell and Hampson, 2006).

2.2 Elastic Impedance

Connolly (1999) pointed out that the generalized term of acoustic impedance for variable incidence angles as a function of offset-dependent reflectivity (Rpp) could be established as Equations 2.4. He called this 'elastic impedance' (EI), and it is valid for small to moderate changes in impedance. It can be expressed as:

$$Rpp(\theta) = \frac{1}{2}\frac{\Delta EI}{EI} \approx \frac{1}{2}\Delta \ln(EI), \qquad \text{(Equation 2.4)}$$

where EI is elastic impedance or angle-dependent impedance.

After applied integration and exponentiation, the function of elastic impedance can also written as:

$$EI(\theta) = Vp^{a}.\, Vs^{b}.\, \rho^{c}, \qquad \text{(Equation 2.5)}$$

where $a = (1+\tan^2\theta)$, $b = (-8K\sin^2\theta)$, $c = (1-4K\sin^2\theta)$, and $K = (Vs^2/Vp^2)$.

In Equation 2.5, Vp and Vs are in m/s and density is in g/cm^3. This EI computation is performed on pre-stack CMP gathers and takes into account the changes in Vp, Vs and density as well as AVO effects. In that process (**Figure 2.4**), CMP gather at the position of well is chosen, variable angle ranges are picked, and then angle stacks or partial stacks are generated based on those ranges. At well with given log curves, elastic impedance trace is computed for different angles of incidence. After that, the comparison between angle-stack traces from gather and those derived from the log curves is performed to obtain adequate EI curve and wavelet extraction for each angle range. The de-convolution is then done using those derived wavelets to invert the

individual angle stacks into elastic impedance volumes. By using EI results especially at far offsets, it provides detailed information on the fluid contents (e.g. Connolly, 1999; Veekan and Silva, 2004).

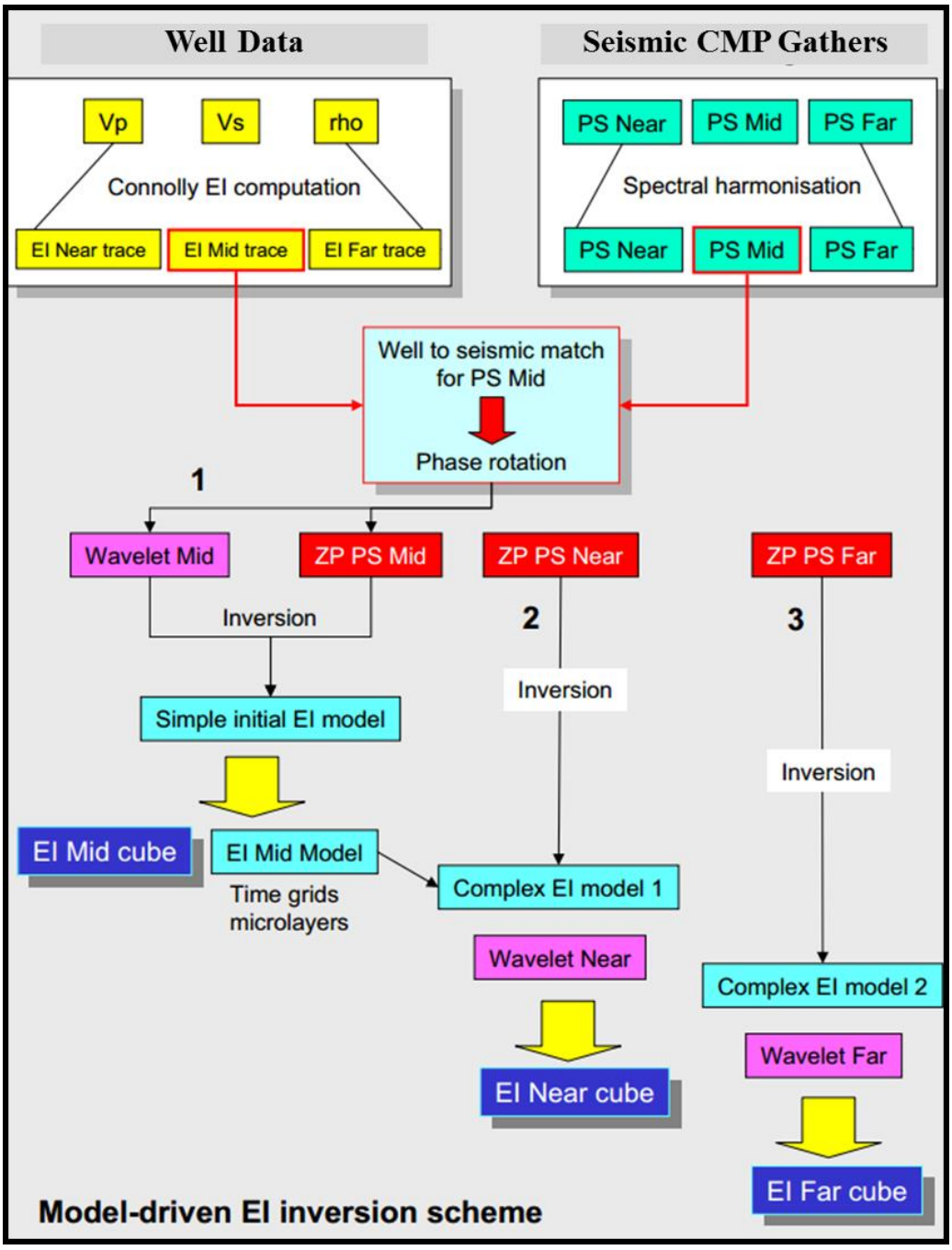

Figure 2.4. Schematic showing the elastic impedance inversion method (modified from Veekan and Silva, 2004).

In contrast, the above EI equation (Equation 2.5) has the problems of unit and dimensions in which the values do not scale correctly for different angles (Whitcombe, 2002). Besides that, sudden drop in angle of incidence (Shi et al., 2014) might conceal the identification of fluid and lithology information across the near-far offset. Whitcombe (2002) introduced the normalization to remove the influence of EI value varies with the angles of incidence.

Firstly, he stated that the EI (Equation 2.5) function's dimensionality varies with incidence angle (θ) and provides numerical values that change significantly with θ (**Figure 2.5**). It is inconvenient for displaying AI and EI together. Eventually, to overcome these problems, the modification of the EI function by using constants Vp_o, Vs_o, and ρ_o was proposed (Whitcombe, 2002). The modified equation can be expressed below:

$$EI(\theta) = (Vp/Vp_0)^a . (Vs/Vs_0)^b . (\rho/\rho_0)^c , \quad \text{(Equation 2.6)}$$

where Vp_0, Vs_0, ρ_0 are the constant in which values might be taken from the averages of those well logs (Vp, Vs, and ρ), then the EI (θ) results will vary around unity (Whitcombe, 2002). Furthermore, more scaling to this function by a factor of $Vp_o.\rho_0$ can provide the same dimensionality in EI and AI which can be written as:

$$EI(\theta) = Vp_o.\rho_0 [(Vp/Vp_0)^a . (Vs/Vs_0)^b . (\rho/\rho_0)^c], \quad \text{(Equation 2.7)}$$

Whitcombe (2002) concluded that for a formation with Vp, Vs, ρ values equal to Vp_o, Vs_o, ρ_o, respectively, the EI in that formation will be the same for the increase of incidence angle with a value of $Vp_o.\rho_0$ (i.e. the acoustic impedance of the formation). These changes of formulation enable a direct comparison between EI values across a range of angles.

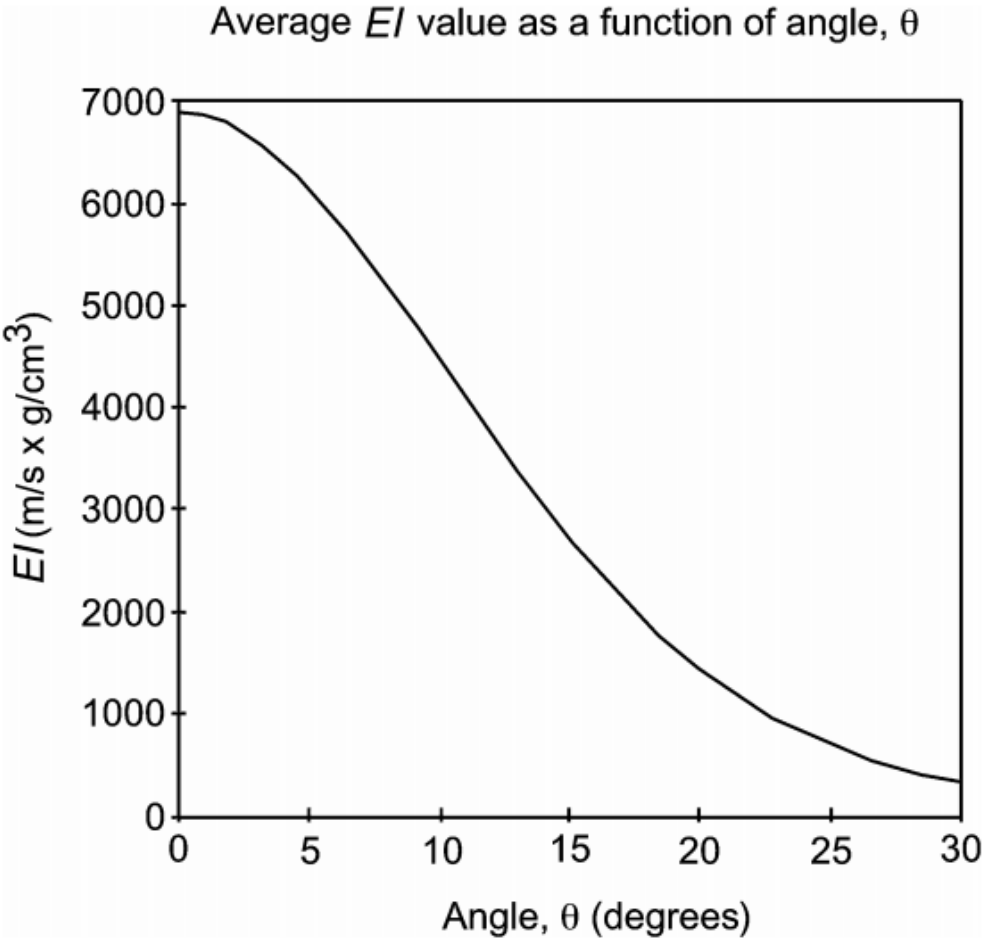

Figure 2.5. An example plot between the average value for the EI logs from one well in the west of Shetland and the range of incidence angle (modified from Whitcombe, 2002).

2.3 Extended Elastic Impedance

The improvement of EI method by replacing the chi (χ) angle instead of angle of incidence (θ) for AVO perspective was introduced by Whitcombe et al., 2002 and they named as extended elastic impedance (EEI). The equation is shown below:

$$EEI\ (\chi) = Vp_0.\rho_0\ [(Vp/Vp_0)^{(\cos\chi+\sin\chi)}.\ (Vs/Vs_0)^{(-8K\sin\chi)}.\ (\rho/\rho_0)^{(\cos\chi-4K\sin\chi)}],$$

(Equation 2.8) where Vp_0, Vs_0, and ρ_0 are normalizing constant representing the averages of P-wave and S-wave velocities and density over the zone of interest or values at the top of the target zone (Whitcombe, 2002). χ is the chi angle.

This approach can define chi angle up to -90° to 90° and make $\sin^2\theta = \tan\chi$ (Whitcombe et al., 2002) as shown in **Figure 2.6**. It provides the same dimensionality of elastic impedance (EI) and correct scale of acoustic impedance (AI).

The variable of chi (χ) angle in EEI function (Eq.2.8) allows computation of impedance value apart from physically observable range of incidence angle (**Figure 2.7**). It includes imaginary angles that might not be recorded in the gather (Shahri, 2013). In the general sense, the EEI log (e.g. Sw, Vp/Vs ratio, Lambda-Rho logs, etc.) at χ=0° is similar to EI log (e.g. Sw, Vp/Vs ratio, Lambda-Rho logs, etc.) at θ=0°, which is the simple form of AI.

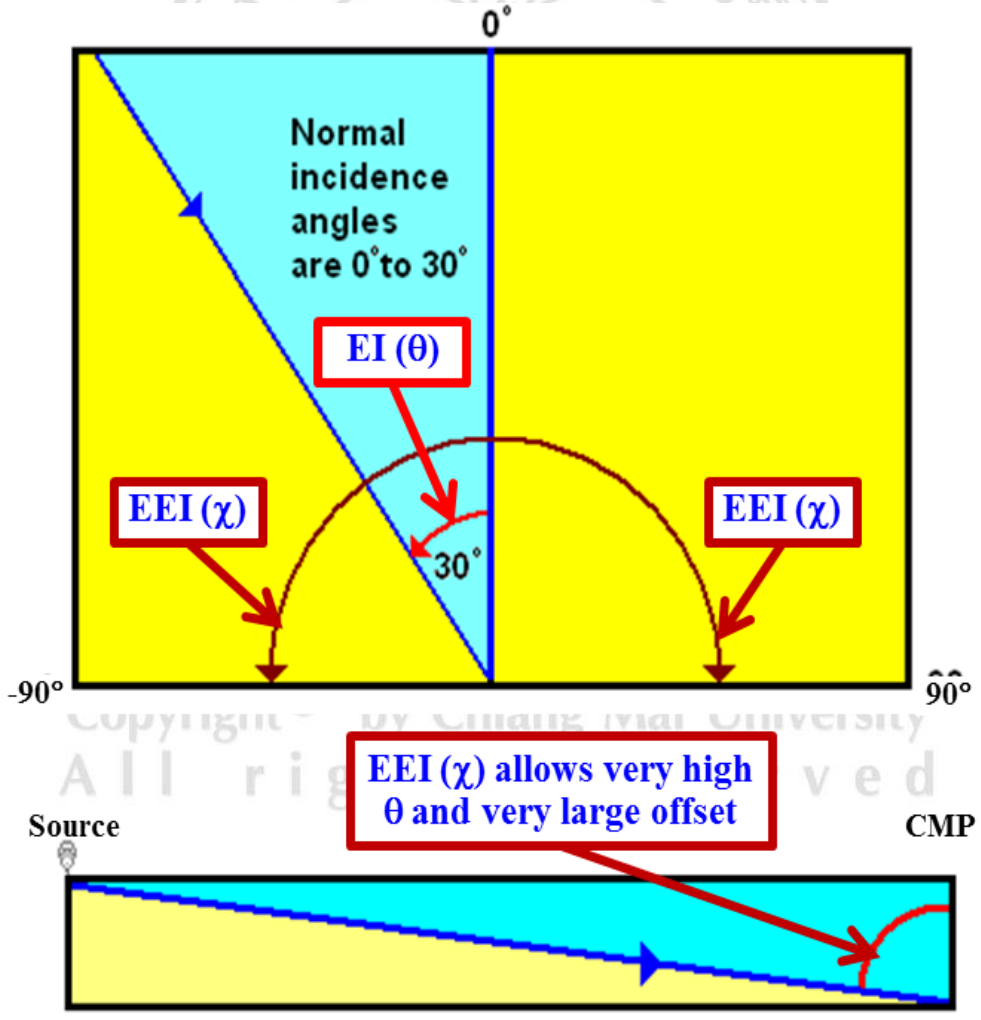

Figure 2.6. The limitation of angle for EI and EEI (modified from Hampson and Russell, 2015).

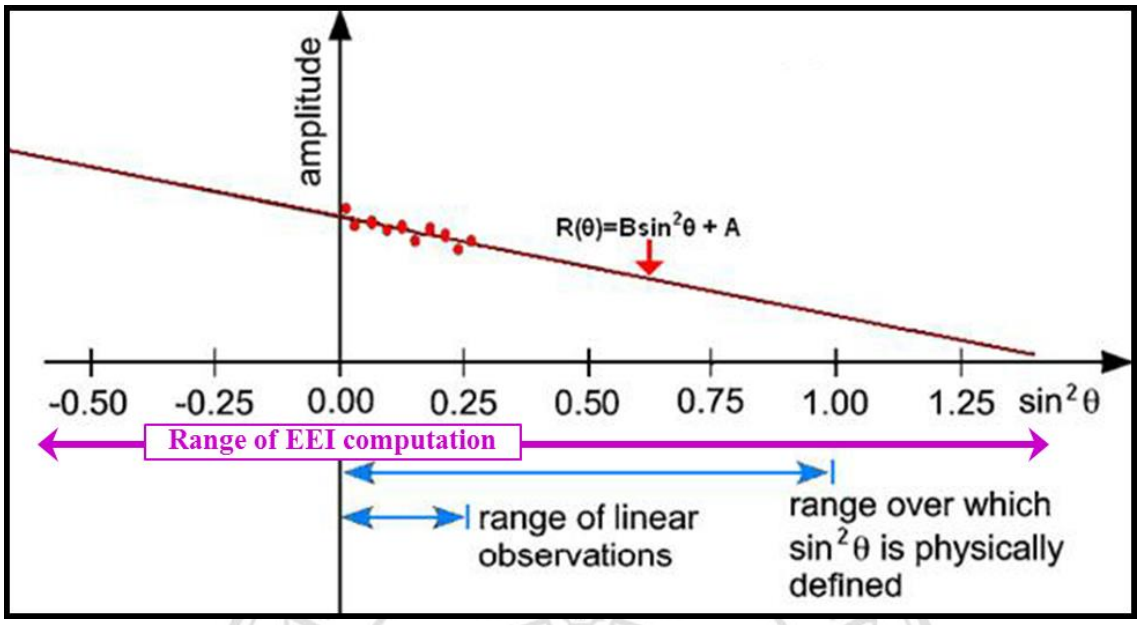

Figure 2.7. The general plot showing conventional and EEI ranges (modified from Hampson and Russell, 2015).

To obtain the optimum chi angle, the process of cross-correlation between target well logs and the range of chi angle would be performed, and then the maximum correlation coefficient corresponding to one chi angle would be achieved. After the achievement of chi angle for either aims of lithology or fluid discrimination, the EEI reflectivity with chosen chi angle will be computed, and then the lithological and/or fluid impedances could be produced later on.

Interestingly, EEI method usually consumes less time than other methods such as simultaneous AVO inversion combined with rock physics inversion or lithology/fluid facies classification studies (Westeng et al., 2014).